# All-Optical Signal Processing Using $\chi^{(2)}$ Nonlinearities in Guided-Wave Devices

Carsten Langrock, *Student Member, IEEE, Student Member, OSA*,
Saurabh Kumar, *Student Member, IEEE, Student Member, OSA*,
John E. McGeehan, *Member, IEEE, Member, OSA*,
A. E. Willner, *Fellow, IEEE, Fellow, OSA*, and
M. M. Fejer, *Fellow, OSA*

*Invited Paper*

***Abstract*—The authors present a review of all-optical signal-processing technologies based on $\chi^{(2)}$ nonlinear interactions in guided-wave devices and their applications for telecommunication. In this study, the main focus is on three-wave interactions in annealed proton-exchanged periodically poled lithium niobate waveguides due to their suitable properties with respect to nonlinear mixing efficiency, propagation loss, and ease of fabrication. These devices allow the implementation of advanced all-optical signal-processing functions for next-generation networks with signal bandwidths beyond 1 THz. In this paper, integrated structures that will allow for improvements of current signal-processing functions as well as the implementation of novel device concepts are also presented.**

***Index Terms*—Dielectric waveguides, nonlinear optics, optical phase matching, periodically poled lithium niobate (PPLN).**

## I. Introduction

THE FABRICATION of low-loss single-mode optical fiber has made possible optical communication links with demonstrated bandwidths exceeding several terahertz. Current optical networks are based on time-division multiplexing (TDM), where multiple relatively low-bit-rate streams of data with the same carrier frequency are interleaved to create a single high-bit-rate stream or wavelength-division multiplexing (WDM), which involves simultaneous propagation of multiple data signals, each at a different wavelength in a single optical line. Although these technologies are individually quite mature, increasing the bandwidth further to allow for new services such as digital television and the next-generation Internet will require the interplay between WDM network topologies [1] and ultrahigh-speed TDM.

WDM systems take advantage of the fortunate coincidence of the low-loss regime of modern optical fibers and the emission cross section of rare-earth-doped fiber amplifiers [e.g., erbium-doped fiber amplifiers (EDFAs)] to provide all-optical amplification, by using data streams with different carrier frequencies. The minimum spacing between these channels is determined by the bit rate of each stream and the need to reduce crosstalk between channels to stay below a desired bit-error rate (BER). By combining TDM and WDM, point-to-point optical links with data capacities close to the theoretical maximum can be designed. To realize this goal, system designers are faced with several challenges critical to the task of interfacing WDM and TDM networks. These include adding/dropping arbitrary channels, resolving wavelength contention, and design of strictly transparent dispersion-compensated links [2], to name a few.

Parametric wavelength conversion has been shown to address these challenges. Optical frequency (OF) mixers can be considered the optical analog to radio frequency (RF) mixers as shown in Fig. 1. Ultrafast highly efficient all-optical gated mixing [3], nearly arbitrary wavelength conversion [4], and spectral inversion for dispersion compensation [5] using OF mixers have been demonstrated by several research groups during the last decade. Applications of nonlinear mixing go beyond simple wavelength conversion because it lends itself to bit-level digital signal processing. Development of optical modules that can assist/replace electronic subsystems that perform simple digital processing functions may be justified if they fulfill any of the following criteria: 1) high-speed operation (scalable beyond 100 Gb/s); 2) parallel operation on multiple wavelength channels; and 3) preservation of information (e.g., phase) carried in the optical domain, usually lost in optical–electronic conversion. Nonlinear mixing satisfies all these criteria and therefore is a suitable platform for development of all-optical digital signal-processing techniques.

This paper is structured as follows. In Section II-A, we give a brief overview of devices for all-optical signal processing

Manuscript received December 15, 2005; revised March 21, 2006. This work was supported in part by the Defense Advanced Research Projects Agency through the University of New Mexico Optoelectronic Materials Research Center under DARPA Prime MDA972-00-1-0024, Intel Corporation, the National Science Foundation under Award 0335110, and Crystal Technology, Inc.

C. Langrock is with the Department of Electrical Engineering, Stanford University, Stanford, CA 94305 USA (e-mail: langrock@stanford.edu).

S. Kumar and A. E. Willner are with the Department of Electrical Engineering, University of Southern California, Los Angeles, CA 90089 USA (e-mail: skumar@usc.edu; willner@commscil.usc.edu).

J. E. McGeehan is with BAE Systems Advanced Technologies, Washington, DC 20037 USA.

M. M. Fejer is with the Department of Applied Physics, Stanford University, Stanford, CA 94305 USA (e-mail: fejer@stanford.edu).

Digital Object Identifier 10.1109/JLT.2006.874605

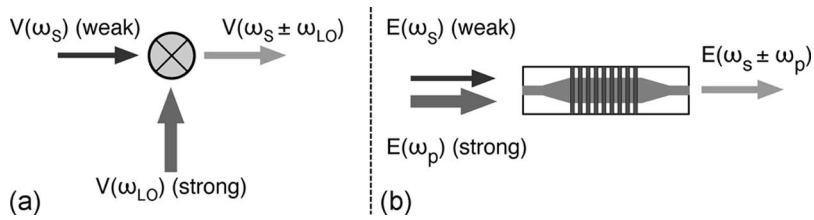


Fig. 1. Comparison between (a) RF and (b) OF mixers.

in $\chi^{(2)}$ media before we introduce the relevant figures of merit with respect to nonlinear processes and guided-wave propagation in Section II-B. Specific examples focus on periodically poled lithium niobate (PPLN) waveguide devices, but other methods are briefly discussed. We describe signal-processing applications in Section III before concluding by giving an overview of novel all-integrated device concepts that will facilitate next-generation signal-processing functionality in Section IV.

## II. Basics

### A. OF Mixers

OF mixers operate in close analogy to RF mixers. In the latter, a strong local oscillator mixes with a (typically) weak signal, producing an output proportional to the product of those two inputs. For quasi-sinusoidal inputs at frequencies $\omega_{\rm LO}$ and $\omega_s$, respectively, the output frequency is $\omega_{\rm out} = \omega_{\rm LO} \pm \omega_s$; the output is related to the inputs by $V_{\rm out} \propto V_{\rm LO} V_s^*$ (for the lower sideband). With a continuous-wave (CW) pump, the carrier frequency is shifted, whereas any amplitude, frequency, and phase information on the envelope is left unchanged. At optical frequencies, similar relationships hold for parametric wavelength converters, so that a strong pump can mix with a weak signal to produce an output at the sum or difference frequency, again preserving the envelope information. Focusing on the difference frequency case most widely used for optical signal processing, $\omega_{\rm out} = \omega_p - \omega_s$, and $E_{\rm out} \propto E_p E_s^*$, as illustrated in Fig. 2(a). With a CW pump, the OF mixer performs wavelength conversion, the optical analog of conventional RF heterodyne mixing, whereas a pulsed pump transforms this device into a gated mixer. Note that the output is proportional to the complex conjugate of the input, so that the mixer also functions as a phase conjugator or spectral inverter.

For a near-degenerate pump frequency, close to twice that of the signal, we can write $\omega_s = \omega_p/2 + \Delta$, and the output is then at $\omega_{\rm out} = \omega_p/2 - \Delta$, i.e., the output is the mirror image of the signal frequency around the degenerate point. With a pump in the vicinity of 775 nm, outputs can be converted from one portion of the C-band to another.

The availability of inexpensive C-band pump sources has led to a frequency conversion technique that does not require a 775-nm pump. This technique relies on the generation of the short-wavelength pump inside the device via second-harmonic generation (SHG) (or sum-frequency generation, SFG) of a suitable C-band source followed by the above-described difference-frequency generation (DFG) between the generated pump and injected signal shown in Fig. 2(b) [Fig. 2(c)], $\omega_{\rm out} = 2\omega_p - \omega_s$ ($\omega_{\rm out} = (\omega_{\rm p1} + \omega_{\rm p2}) - \omega_s$). Such a process requires the cascaded execution of two $\chi^{(2)}$ processes (SHG/SFG followed by DFG) and has therefore been termed a cascaded $\chi^{(2)}$ process, sometimes written as $\chi^{(2)} : \chi^{(2)}$ [6]–[8]. Viewed as a black box, such a device effectively acts as a four-wave mixer (FWM) with a large effective $\chi^{(3)}$. Due to the short device length on the order of several centimeters, this quasi-FWM interaction is essentially free of parasitics such as stimulated Brillouin scattering (SBS) and other undesired interactions encountered in true $\chi^{(3)}$ nonlinear devices.

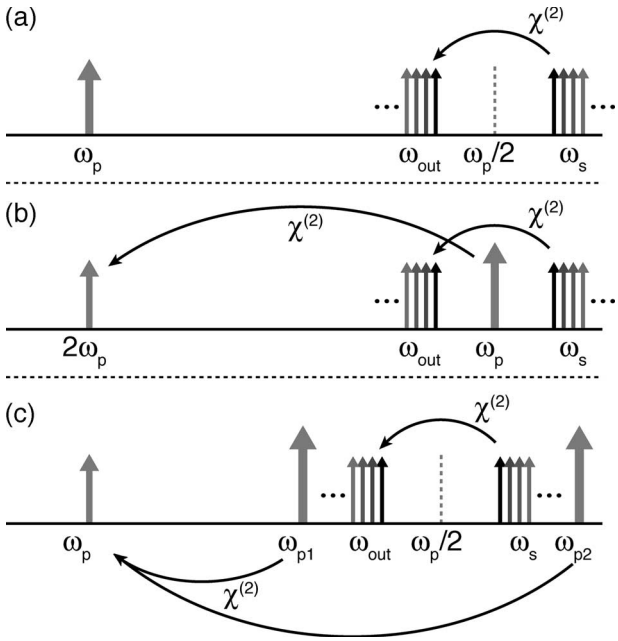


Fig. 2. Schematic description of (a) difference-frequency mixing between a strong pump at $\omega_p$ and a signal at $\omega_s$, (b) cascaded second-order nonlinear frequency mixing with single pump via SHG, and (c) with two pumps via SFG.

### B. Basic Device Considerations

The difficulty in implementing OF mixers arises from the weak nonlinearities in available materials. The mixers are, of necessity, long compared with the wavelength of the interacting radiation, requiring matching of the phase velocities of the fields at different frequencies participating in the interaction. Even with phase-velocity matching, the pump power required for efficient operation is prohibitive in conventional bulk nonlinear media. The use of highly nonlinear materials, like PPLN or AlGaAs, together with the confinement provided by guided-wave geometries, can increase the efficiency by several orders

of magnitude over that available in bulk interactions, reducing the required pump powers to the range of 10–20 dBm [9].

In the low-gain and nondepleted pump limit (which will be assumed unless otherwise stated), the output power generated in a DFG interaction in a waveguide of length $L$ can be written as $P_{\rm out} = \eta_{\rm nor} L^2 P_p P_s$, where the normalized efficiency $\eta_{\rm nor}$ $[\mathrm{W}^{-1} \cdot \mathrm{cm}^{-2}]$ is independent of length and power and depends on the nonlinear properties of the medium and the overlap of the interacting waveguide modes [10], [11]. The output grows quadratically with the length of the device, is proportional to the pump power, and, at fixed pump power, is linear in the signal input power; signal dynamic ranges $> 50$ dB have been demonstrated and are only limited by quantum noise and pump depletion. For cascaded operation, there are two nonlinear conversion steps: pump to second harmonic, followed by second harmonic and signal mixing to generate the output. Under the same conditions, the output power can be written as $P_{\rm out} = (\eta_{\rm nor} L^2 P_p/2)^2 P_s$. More detailed discussions including effects of loss and pump depletion can be found in [8], [12], and [13].

The output power of a DFG device is reduced in the presence of nonzero phase-velocity mismatch by a factor $\mathrm{sinc}^2(\Delta k' L/2)$, where $\Delta k' = |k_p - k_s - k_{\rm out}|$, and $k_i = 2\pi n_i/\lambda_i$ $(i = p, s,$ or out; $\lambda_i \equiv$ vacuum wavelength, $n_i \equiv$ effective index). Rather than true phase-velocity matching, the quasi-phasematching (QPM) method, in which a periodic microstructure in the medium compensates for the velocity mismatch of the interacting waves, has proven to be more effective in most practical signal-processing devices. In an ideal QPM device, the microstructure exhibits a periodic sign change in the nonlinear susceptibility with a period $\Lambda_g$ chosen so that the spatial frequency $K_g = 2\pi/\Lambda_g$ satisfies $K_g = \Delta k'$, and the interaction proceeds with an effective wavevector mismatch $\Delta k = \Delta k' - K_g$. The most common means for implementing this sign change is through periodic poling of a ferroelectric medium like lithium niobate or through orientation pattering of a semiconductor like AlGaAs, as discussed subsequently. The power of the QPM approach is that it allows the use of interactions that could not otherwise be phasematched, e.g., those using copolarized pump and signal to take advantage of the largest nonlinear tensor component in $LiNbO_3$, or those in isotropic media like AlGaAs. Furthermore, the tuning behavior can be engineered through the use of aperiodic QPM gratings, as is discussed in Section II-D.

An important parameter of the mixing process is the bandwidth around the phasematched wavelength $\lambda_0$. As a result of the $\mathrm{sinc}^2(\Delta k L/2)$ dependence, the output falls to half of its phasematched value when $\Delta k \approx \pm 0.89\pi/L$. For tuning of a signal near degeneracy at a fixed pump wavelength, $\Delta k$ increases only quadratically with detuning. The bandwidth then depends only on $1/\sqrt{L}$, and large bandwidths are obtained (typically 70-nm full-width at half-maximum (FWHM) bandwidth in 5-cm-long PPLN devices, see Fig. 6). Tuning the pump at a fixed signal wavelength leads to a linear variation of $\Delta k$ with tuning and, hence, leads to a linear dependence of the bandwidth on $1/L$. In this case, the bandwidths are rather narrow (typically 0.2 nm for a 5-cm-long PPLN device). Techniques for using engineered QPM gratings or devices with two pump wavelengths to evade this limit are discussed in Section II-D.

### C. Device Technology

Guided-wave frequency conversion devices have been studied since the early days of nonlinear optics [14]. Interest in blue light sources for high-density optical data storage and the availability of high-power near-infrared (NIR) semiconductor lasers motivated significant engineering developments, especially QPM ferroelectric waveguide devices in the late 1980s and early 1990s [9], [15], [16]. This progress served as a base for the first demonstrations of signal-processing devices for telecommunications applications in periodically poled ferroelectrics [11], [17]–[20] and parallel developments in orientation-patterned semiconductor waveguides [21], [22]. In this paper, we focus on the ferroelectric devices.

The essential parameters that describe a simple waveguide frequency-mixing device are the conversion efficiency as a function of pump power and the conversion bandwidth. The former depends on several factors, including the normalized efficiency $\eta_{\rm nor}$, the length of the device, the passive insertion loss (a combination of pigtailing and propagation losses), and the homogeneity of the structure. The length and homogeneity also determine, along with intrinsic material properties, the bandwidth of the device. There are clearly tradeoffs between these factors, as for example, longer devices have higher efficiencies but narrower bandwidths and stricter fabrication tolerances, and more tightly confining waveguides have higher normalized efficiencies, but higher propagation losses. To illustrate these factors, we first discuss proton-exchanged (PE) PPLN waveguide devices as perhaps the most widely used example, then compare them with other common material systems.

The fabrication of QPM waveguide devices can be divided into two independent processes, namely, 1) the generation of the QPM grating via poling of the ferroelectric substrate and 2) the formation of the guiding structure, typically by an indiffusion process.

Fig. 3 shows a typical PE PPLN process [23]. The inversion of the ferroelectric domains on a single-domain $z$-cut $LiNbO_3$ wafer can be achieved in several ways [24]. By far, the most widely used method today is electric-field poling, in which a high-voltage pulse is applied to electrodes lithographically patterned on the surface of the wafer. Domain reversals are induced in the area under the electrodes, so that both simple periodic patterns or complex aperiodic patterns can be fabricated with comparable ease. Typical QPM periods for 1.5-$\mu$m-wavelength operation are around 16 $\mu$m.

After electric-field poling, the formation of waveguides requires a second lithography step in which channels are defined along the crystallographic $y$-direction on top of a silicon dioxide mask sputtered on the $+z$ side of the wafer. Lithium ions are exchanged with hydrogen ions in the channels by placing the wafer into a heated benzoic acid bath. Subsequent high-temperature annealing diffuses the protons deeper into the substrate, increasing the effective nonlinear coefficient, which is found to be almost zero in the as-exchanged $H_xLi_{1-x}NbO_3$

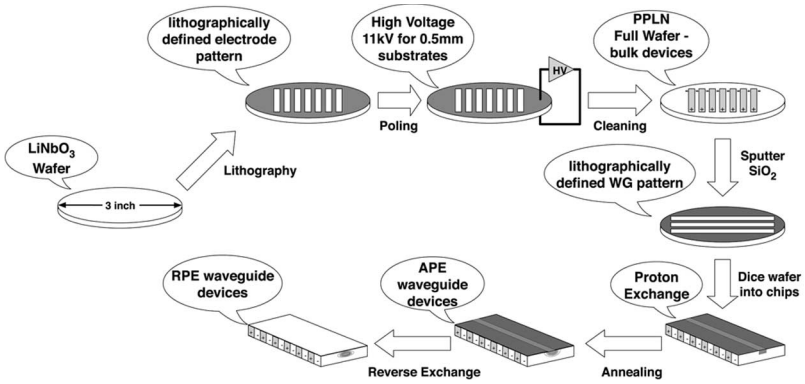


Fig. 3. Bulk, APE, and RPE PPLN processing chart.

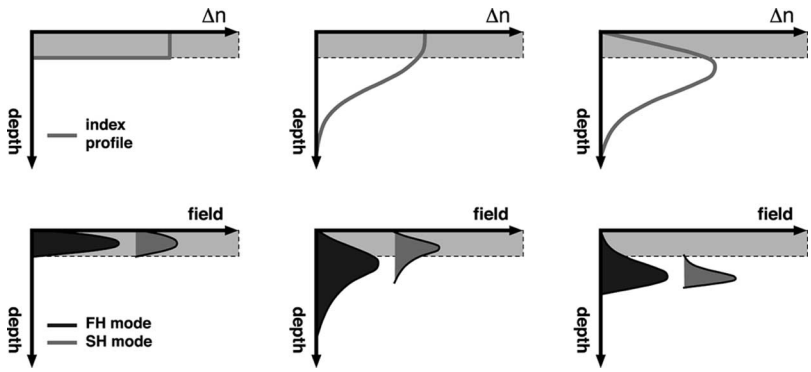


Fig. 4. Comparison between PE, APE, and RPE indexes and mode profiles in the depth dimension. The gray layer represents the as-exchanged step index profile, which is found to have a greatly reduced nonlinearity.

film ("dead layer") [25], [26], and reducing the propagation losses by pushing the propagating fields farther from the substrate surface (see Fig. 4). The waveguides formed by this two-step process are termed annealed PE (APE) waveguides and have been successfully used by many groups. Many of the early signal-processing demonstrations were based on APE PPLN devices. Typical values of $\eta_{\rm nor}$ in APE waveguides are 0.4 $W^{-1} \cdot cm^{-2}$, so that for a 5-cm-long device, efficiencies of 10 $W^{-1}$ can be obtained; propagation losses of 0.3–0.4 $cm^{-1}$ are typical [27].

Due to the asymmetric APE refractive index profile along the depth dimension, the peaks of the interacting modes at different wavelengths are not well aligned with respect to each other, reducing the overlap integral and hence the maximum normalized efficiency (see Fig. 4). The index profile can be buried to create a more symmetric waveguide by an additional exchange step in a lithium-rich melt, replacing protons by lithium ions in the top layer of the waveguiding structure [28], [29]. This reverse PE (RPE) step also increases the separation between the propagating fields and the substrate surface, further decreasing the propagation losses. Typical values of $\eta_{\rm nor}$ in RPE waveguides are 1 $W^{-1} \cdot cm^{-2}$, so that for a 5-cm-long device, efficiencies of 25 $W^{-1}$ can be obtained; propagation losses of 0.1–0.2 dB/cm are typical [30].

Several considerations enter into the device design besides normalized efficiency and propagation loss. Essential to reliable high-yield fabrication of either APE or RPE waveguides are so-called noncritical designs [10], [31], for which there is no

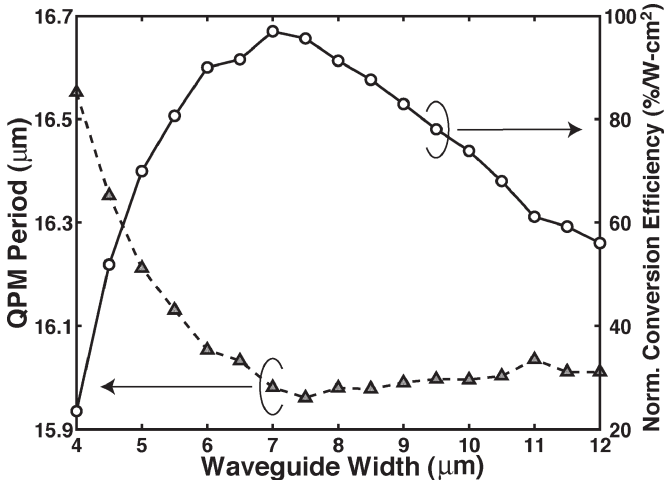


Fig. 5. Simulation results showing the noncritical waveguide width for which there is no first-order dependence of phasematching wavelength on waveguide dimensions.

first-order dependence of phasematching wavelength on waveguide dimensions (see Fig. 5). Such designs are more tolerant of small errors in lithography and thermal processing, which otherwise tend to broaden and reduce the peak value of the phasematching curves. Another important consideration is convenient low-loss coupling to single-mode fibers (SMFs), which requires a taper between the tightly confining mixing regions (typical mode sizes $6 \times 4.5$ $\mu$m) to a size matched to

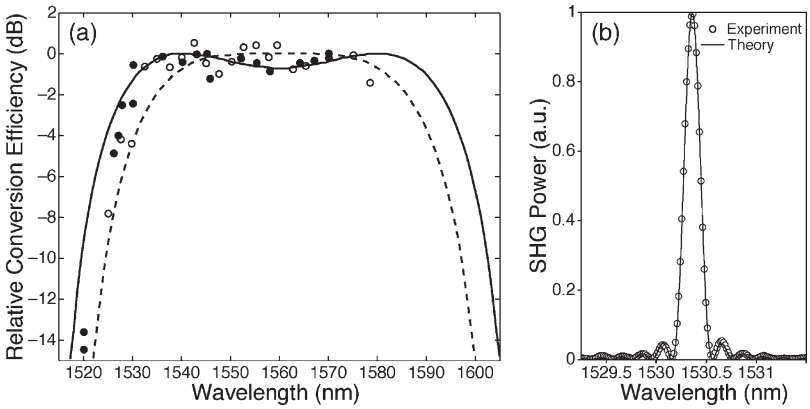


Fig. 6. (a) Efficiency versus signal wavelength for fixed pump wavelengths in a 41-mm-long difference frequency mixer; dashed gray curve and open circles correspond to degenerate operation (56-nm bandwidth), whereas solid black curve and filled circles show broadened response due to pump detuning (78-nm bandwidth) [34]. (b) SHG tuning curve of a PPLN waveguide device with a 5-cm-long QPM section.

standard SMF with a mode-field diameter of $\sim 10.5\ \mu$m. Mode-mismatch losses are under 0.4 dB. Both segmented waveguides and continuous tapers have been used successfully [32]. Precise models of the concentration-dependent diffusion of protons and the wavelength-dependent refractive index induced are essential for this sort of design [33].

Overall, the best current RPE waveguides have $\eta_{\rm nor} \geq 1\ \mathrm{W}^{-1} \cdot \mathrm{cm}^{-2}$, propagation losses of $\leq 0.1$ dB/cm, and pigtailing losses of $\leq 0.4$ dB, so that conversion efficiencies $\geq 3.5\%$/mW have been obtained. DFG signal bandwidths in excess of 70 nm and SHG transfer functions matching theoretical predictions closely have been demonstrated (see Fig. 6).

A number of other material systems are being investigated for signal-processing applications. One aspect of APE and RPE PPLN waveguides that has caused difficulty is the so-called photorefractive damage (PRD), which are changes in the refractive index induced by the presence of visible and NIR radiation. Operation at elevated temperatures greatly reduces these effects; depending on power levels, 80 °C–120 °C operation is common. Alternative PRD-resistant substrates (MgO:$LiNbO_3$ and ZnO:$LiNbO_3$) and waveguide dopants (Zn) have been used [35]–[38], as have mechanically defined waveguides not requiring any indiffused dopants [39], [40], which have allowed room-temperature operation with typical values of $\eta_{\rm nor} = 0.4\ \mathrm{W}^{-1} \cdot \mathrm{cm}^{-2}$ and propagation losses of $< 1$ dB/cm. Ti-indiffused waveguides in PPLN have been fabricated with more loosely confining modes, leading to lower propagation losses ($< 0.1$ dB/cm) and lower $\eta_{\rm nor}$ $(0.2\ \mathrm{W}^{-1} \cdot \mathrm{cm}^{-2})$ [41]. Devices as long as 20 cm have been fabricated in these latter waveguides [42].

### *D. Device Limitations and Solutions*

Two issues that emerge in the basic performance of PPLN devices are the single-polarization nature of the devices and the narrow bandwidth for pump tuning.

The single-polarization operation results both from the highly anisotropic nonlinear susceptibility of $LiNbO_3$ and, for PE devices, that the waveguides support only a single polarization. Several approaches have been taken to address this problem. Polarization diversity approaches, either with two waveguides or with counterpropagating waves in a single waveguide, have been demonstrated successfully in APE PPLN waveguides [43], [44], as has a scheme with a single waveguide incorporating a polarization rotator in Zn-doped PPLN waveguides [39]. The high symmetry of the nonlinear susceptibility of AlGaAs combined with ridge waveguides engineered to phasematch both polarizations simultaneously has allowed true polarization-independent operation [22].

Several schemes have also been used to evade the limitations imposed by the narrow pump-tuning bandwidth characteristic of $\chi^{(2)}$ parametric converters. With two tunable pump lasers, the scheme shown in Fig. 2(c) is possible, where one of the pumps sums with the input to generate the allowed intermediate frequency, and the second pump mixes with the intermediate frequency to generate the desired output frequency. In this way, any input wavelength can be converted to any output wavelength within the $\sim$ 70-nm bandwidth of the PPLN device [4]. Another approach takes advantage of the engineerability of QPM gratings, most easily visualized in the spatial Fourier domain. A periodic QPM grating of length $L$ designed to quasi-phasematch wavelength $\lambda_0$ contains a single fundamental spatial frequency component, broadened by an amount inversely proportional to the finite length $L$. It is this broadening that allows phasematching of a narrow range of wavelengths in the vicinity of $\lambda_0$. A grating containing multiple Fourier components, obtained for example by imposing a periodic phase-reversal sequence on the basic periodic grating, will contain a QPM peak associated with each Fourier component. Each peak then allows operation with a different pump wavelength. Fig. 7 shows experimental results for a series of such designs [45]. More general Fourier synthetic design approaches allow fairly general control over the amplitude and phase of the transfer function of the QPM device [46].

Although the system applications described in Section III as well as the device concepts outlined in Section IV have been implemented using PE or RPE PPLN waveguide devices, we note that these examples are, for the most part, independent of the waveguide technology used and could as well be realized, for example, in Ti-indiffused QPM waveguide devices.

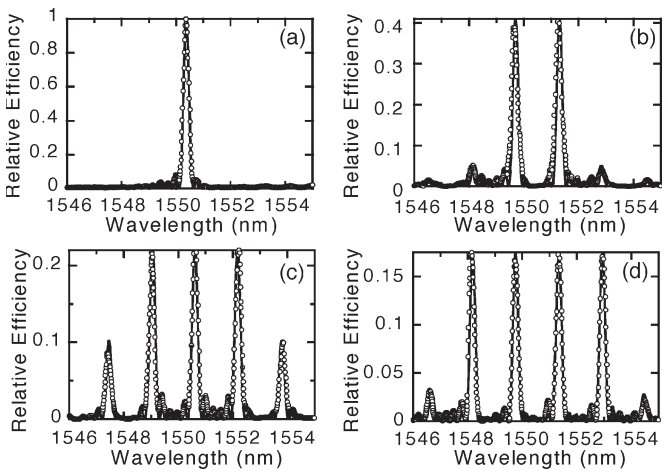


Fig. 7. SHG wavelength-tuning curves for (a) one-channel device, (b) two-channel device, (c) three-channel device, and (d) four-channel device. Circles are measured results, whereas solid lines are theoretical fits. Efficiencies are relative to the peak efficiency of a one-channel device.

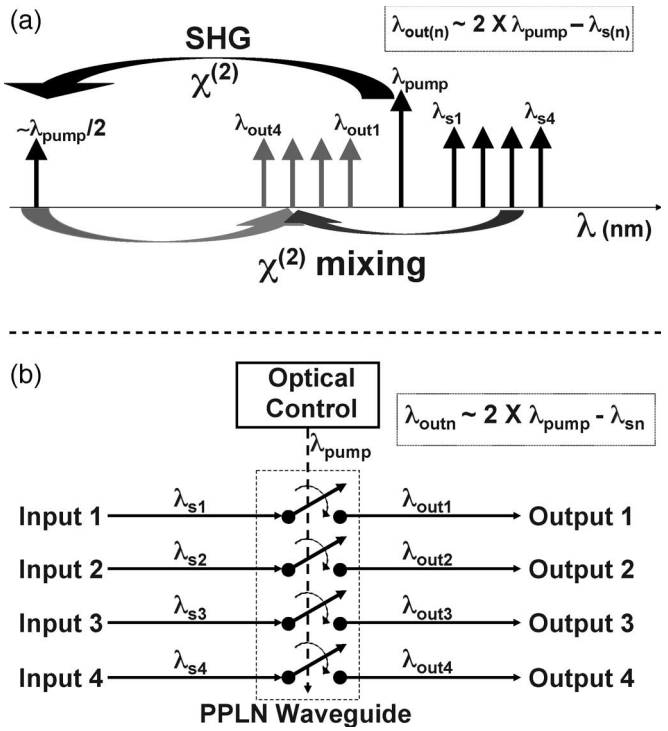


Fig. 8. (a) Single-pump operation of a PPLN waveguide. Each input is individually wavelength-converted through the process of SHG/DFG. (b) This switching behavior corresponds to a multipole single-throw switch, where individual inputs are transferred to the corresponding outputs if the control is turned on.

Long-haul high-speed communications experiments have recently been demonstrated using Ti-based PPLN waveguide subsystems [47], [48].

## III. System Applications

From a system designer's perspective, a single-pump PPLN waveguide can operate as an optically controlled multi-pole single-throw switch. This means that there can be several inputs, which are individually transferred to their corresponding

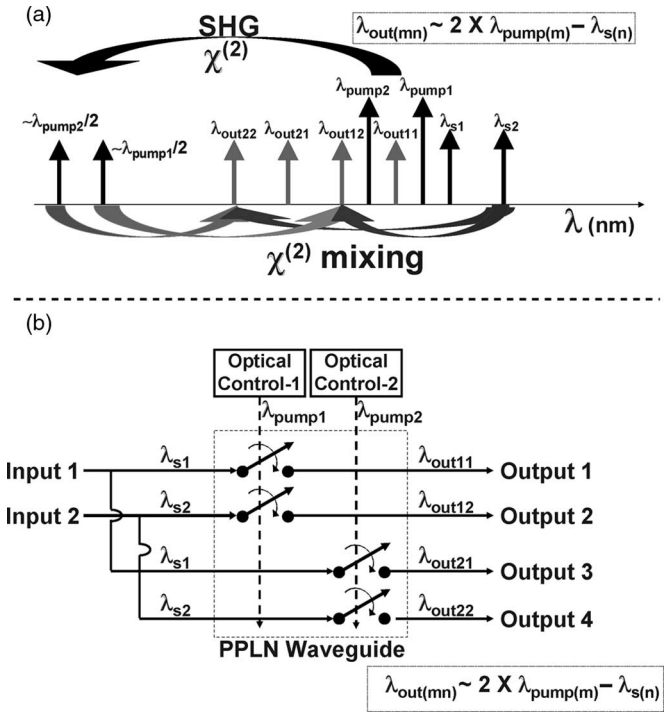


Fig. 9. (a) Multipump operation of a PPLN waveguide. Each input is wavelength-converted to two outputs (governed by the two pump wavelengths) if the pumps are on. (b) This switching behavior corresponds to a multipole multithrow switch, where individual inputs can be transferred to multiple outputs if the corresponding controls are turned on. The specific example in the figure refers to a case of two inputs and two pumps.

outputs, when the optical control signal (the PPLN waveguide's pump) turns on, as shown in Fig. 8. Inasmuch as the inputs and outputs are identified by their wavelengths, PPLN waveguides can operate on multiple WDM channels simultaneously. As mentioned earlier, a PPLN waveguide may be designed for operation with multiple pumps. In such a device, several inputs can be directed to a set of outputs (determined by the set of pump wavelengths), each individually controlled by the different control signals (pumps). This switching action corresponds to a multi-pole multi-throw switch, as depicted in Fig. 9. It is possible to have multiple outputs emerge at the same wavelength if the input wavelengths are chosen appropriately. Optical switching in a PPLN waveguide has several attractive properties, including 1) quantum-limited spontaneous emission noise; 2) no added chirp; 3) wide operational bandwidth ($>$ 70 nm); 4) ultrahigh-speed operation ($>$ 1 THz); 5) similar up- and down-conversion efficiencies; and 6) multichannel operation with minimal crosstalk. As described in Section II-A, the nonlinear processes in the PPLN waveguide lead to phase conjugation [49] of the input signal. This spectral inversion with respect to the PPLN waveguide's pump wavelength can prove useful for several applications including chromatic dispersion compensation [5], [47], [48], [50], [51]. Moreover, because the wavelength conversion process preserves the phase relationship between data bits, it can be used for phase-coded signals, e.g., differential phase-shift keying (DPSK) and quadrature phase-shift keying (QPSK).

The rest of this section reviews some of the applications of PPLN waveguides and highlights recent experimental

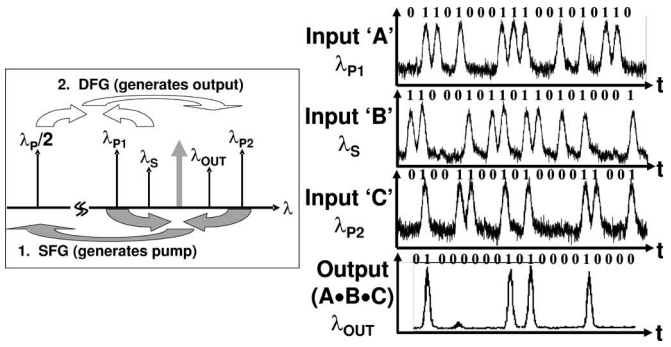


Fig. 10. Operation of a three-input AND gate. SFG between two of the inputs generates a product at the PPLN pump wavelength, which then mixes with the third input via DFG, leading to a wavelength-converted output that represents the logic AND of all three inputs.

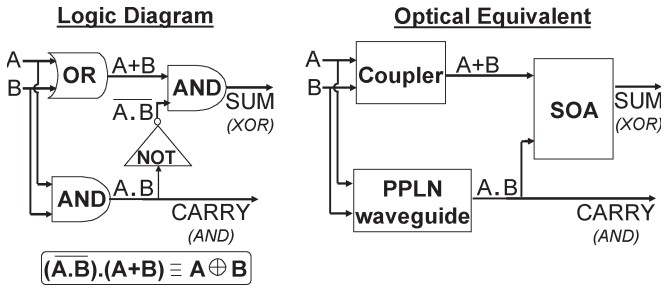


Fig. 11. Two-stage XOR-less design for an all-optical half-adder. The first stage is a PPLN waveguide-based AND gate that generates the carry output. This output also drives the second nonlinear stage (an SOA) to generate the sum output.

demonstrations of various signal-processing subsystems that have been enabled using them. This section is divided into three parts. Section III-A focuses on digital optical signal processing using PPLN waveguides, Section III-B surveys phase-based signal processing, and Section III-C looks at some miscellaneous applications.

### A. Digital Signal Processing

Inasmuch as a PPLN waveguide performs wavelength conversion of an input signal only when the pump is on, the process can be thought of as a logic AND operation between the pump and signal. This property has been exploited to enable various all-optical digital processing modules.

The cascaded $\chi^{(2)}$ processes, namely, SFG and DFG that occur simultaneously in a PPLN waveguide, have been used to develop a three-input AND gate. Such a gate performs the AND operation on two optical inputs while controlling the logic operation with a third optical input. Two of the input wavelengths undergo SFG to generate a pump at the OF mixer's phasematching wavelength, which then mixes with the third input to generate a wavelength-converted output. Experimental results from a recent demonstration [52] are shown in Fig. 10.

PPLN waveguides have also been used as AND gates as part of larger optical signal-processing units. For example, an all-optical half-adder comprises an AND gate and an XOR gate to generate the carry and sum outputs, respectively. However, a modified design for a half-adder can eliminate the XOR gate, thereby simplifying the optical setup. As shown in Fig. 11, this

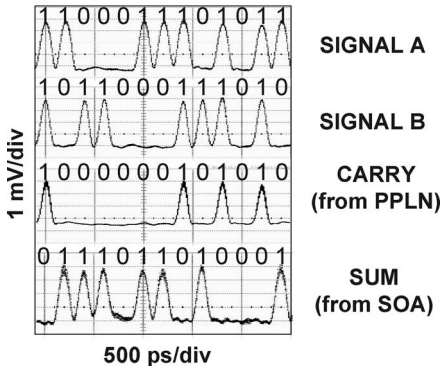


Fig. 12. Waveforms from a PPLN waveguide-based half-adder. The carry output is obtained from a PPLN waveguide, and the sum output is obtained from an SOA.

design requires the output of the AND gate to be fed to another nonlinear optical element. The PPLN waveguide is very well suited for the AND operation in such a design because it only adds minimal noise and provides a high-quality output to be used in the second nonlinear element. Waveforms showing the experimental results from a 5-Gb/s all-optical half-adder [53] that uses a PPLN waveguide as an AND gate are shown in Fig. 12. As is clearly visible, the carry output exhibits a high extinction and signal-to-noise ratio (SNR).

As single-channel data rates keep increasing, electronic processing of data packets at routers in an optical network and the required optical–electronic–optical conversions may present a speed bottleneck. Therefore, one of the primary motivations for developing optical signal-processing techniques is to assist/replace some of the electronic modules used in network routers to perform various processing tasks on data packets [54], [55]. For example, packet-switched networks require a mechanism to prevent "routing loops," without which mislabeled or misdirected packets may circulate endlessly, leading to severe network congestion [56]. The conventional technique used is to include a binary field called the time-to-live (TTL) field in each packet's header. The TTL represents the number of network-hops the packet can go through before being dropped. Each router decrements the TTL by 1 before forwarding the packet onto the next node. To keep the packets in the optical domain and avoid slow electronic processing, routers may benefit from all-optical implementations of a TTL processing module. One such demonstration has been conducted using cross-gain modulation (XGM) in a semiconductor optical amplifier (SOA) to generate an inverted copy of the original TTL followed by a pair of PPLN waveguides operated in tandem to selectively transfer bits from the original and inverted copies to imitate the decrementing process [57]. Fig. 13 explains the synchronized operation of the PPLN waveguides to achieve data replacement through wavelength conversion. Successful decrementing of an 8-bit TTL field in a 10-Gb/s non-return-to-zero (NRZ)-modulated packet's header has been achieved with $< 2.5$-dB power penalty.

Another processing step that requires a field to be updated by replacing part of the packet's header on the fly is "label swapping" [58]–[60]. To efficiently and transparently route packets to an appropriate destination, optical networks may

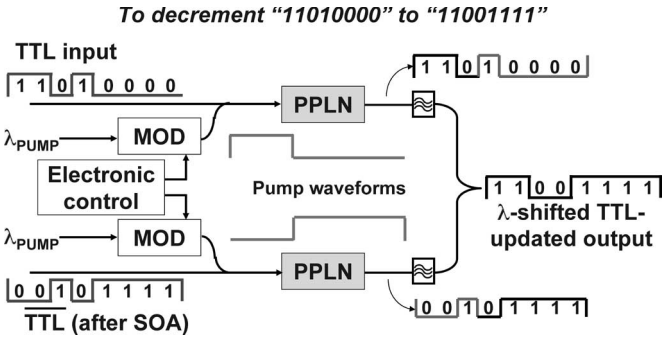


Fig. 13. Conceptual diagram of TTL decrementing using selective switching in PPLN waveguides. XGM in an SOA is used to generate an inverted copy of the TTL field. The PPLN pumps are individually modulated to $\lambda$-shift the inverted TTL up to and including the first one bit and to $\lambda$-shift the original TTL at other times.

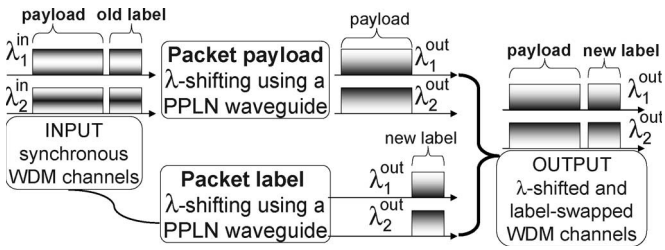


Fig. 14. Concept of all-optical label swapping using PPLN waveguides. One of the waveguides is used to selectively $\lambda$-shift the payload, whereas the other $\lambda$-shifts the new label. The new label is coupled with the payload to generate a wavelength-converted and label-swapped packet.

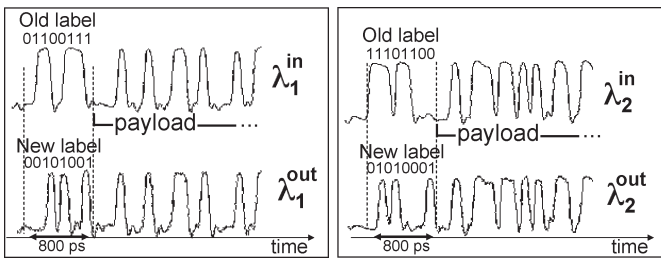


Fig. 15. Multichannel label swapping using selective switching in PPLN waveguides. Packets on two different wavelengths can be simultaneously processed in the PPLN waveguide with their respective labels being replaced independently with new ones.

require the use of labels, as proposed in multi-protocol label switching (MPLS) [61], [62]. Labels need to be read at the routers to determine the output port for the packet. Label swapping is also required to update the information carried in the label for the next router node. To limit the load on electronic processing modules, all-optical techniques to rewrite labels (label swapping) are being explored. Several techniques have been proposed [63]–[66] for label swapping, most of which rely on wavelength conversion. The PPLN waveguide provides the opportunity for label swapping of multiple channels via selective conversion of the payloads to erase the labels, followed by the addition of the new labels at the new wavelengths. A demonstration of this technique on two WDM channels at 10 Gb/s (conceptually explained in Fig. 14) has been reported [67] that introduced $<$ 2.5-dB power penalty. The waveforms in Fig. 15 show the label-swapped packets.

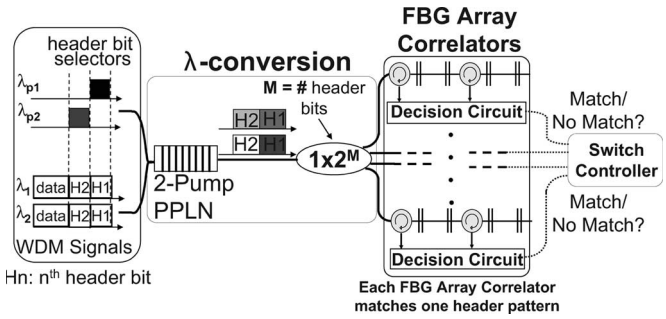


Fig. 16. Concept of WDM header recognition using multipump PPLN waveguide. By using modulated pumps, each header bit of each input channel can be mapped onto a different wavelength. These $\lambda$-shifted bits can be compared with preset header patterns using optical correlators.

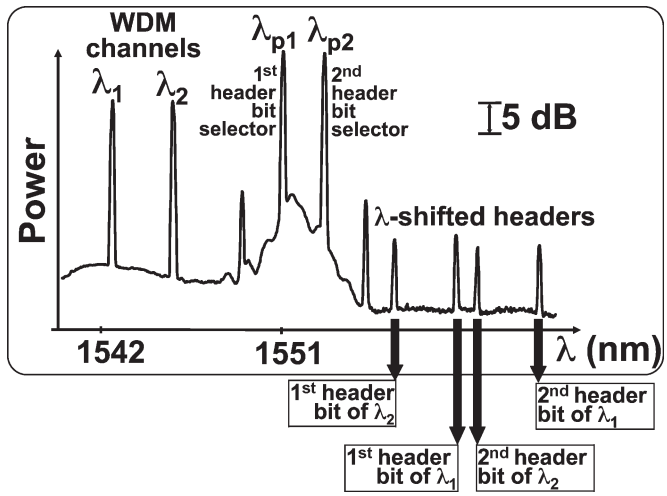


Fig. 17. Wavelength conversion spectrum obtained in a two-channel, two-bit header recognition module using a two-pump PPLN waveguide. Each input header bit is mapped onto a new wavelength, leading to a total of four output wavelengths.

Multi-pump PPLN waveguides have been used to enable simultaneous multi-channel all-optical header recognition [68]. Using modulated pumps, offset by a bit time, each bit of the incoming channels' headers can be converted to individual output wavelengths. The wavelength-converted bits obtained through this process of "time-to-wavelength" mapping can be compared with preset header patterns using fiber-Bragg-grating (FBG)-based correlators. The concept of such a scheme for two data channels with two-bit headers is shown in Fig. 16, and the experimentally observed wavelength conversion spectrum is shown in Fig. 17. An experimental demonstration of switching using this PPLN-based WDM header recognition technique with $<$ 1-dB power penalty has been reported [68].

The ability to perform wavelength conversion at bit-time scales using PPLN waveguides has been exploited to implement several other processing modules. One such demonstration involved time-slot interchange (TSI) between two TDM channels. In a TDM network, the time slot occupied by a signal determines its output port at a switching node. Therefore, to switch the signal to a different output port (and thus, change its destination), its time slot needs to be changed. This process is called TSI [69]. All-optical swapping of adjacent time slots at 2.5 Gb/s has been demonstrated [70] using a three-step process

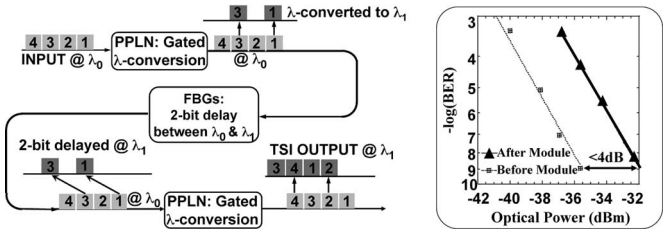


Fig. 18. TSI between two TDM channels using PPLN waveguides. Data bits corresponding to one time slot are wavelength-shifted and delayed before being combined with the bits from the other slot.

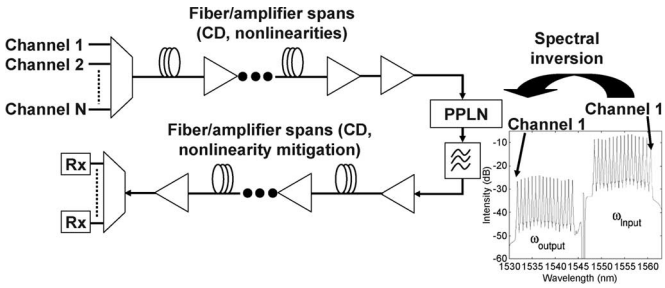


Fig. 19. Generic setup for midspan spectral inversion and phase conjugation using a PPLN waveguide. The PPLN waveguide "inverts" the OF spectrum, allowing the dispersion of the second half of the link to counterbalance that of the first half (copyright IEEE 2004).

in which 1) a PPLN waveguide-based wavelength converter places the odd-numbered bits onto a new wavelength; 2) FBGs introduce a two-bit delay between wavelengths; and 3) another wavelength converter places the non-delayed even-numbered bits onto the new wavelength. This process is explained in Fig. 18, and the BER curves are also presented.

### *B. Phase-Based Signal Processing*

A useful property of PPLN waveguides is their phase-preserving nature; the output signal retains the phase properties of the input signal while introducing negligible optical SNR (OSNR) degradation. This allows SHG and wavelength conversion that can be controlled at bit-time scales without destruction of phase information.

There have been a number of recent reports on the use of phase conjugation in a PPLN waveguide to mitigate signal degradation resulting from chromatic dispersion [5], [47], [48], [50], [51], [71] and nonlinear effects [72] within optical fiber. A generic setup for such a mitigator is shown in Fig. 19. The PPLN waveguide-based phase conjugator is placed at the midpoint of a long fiber link. After wavelength conversion, the optical spectrum and phase of the signal are inverted. Thus, the second half of the fiber link effectively cancels out the degradations introduced by the first half. In one such demonstration, a PPLN waveguide wavelength converter was used for midspan spectral inversion in a 40-Gb/s transmission system, compensating for chromatic dispersion effects over 800 km of SMF. Sixteen WDM channels, each modulated with a $2^{31}-1$ pseudorandom binary sequence (PRBS) at 40 Gb/s, were transmitted through four fiber spans, each span consisting of 100-km SMF and an EDFA. At this point, a PPLN waveguide was inserted following which the signal traveled through another set of four identical spans to the receiver. Whereas each SMF span induced a positive dispersive effect on the transmitted signals, the spectral inversion resulting from the PPLN waveguide in conjunction with the positive dispersion from the second set of fiber spans nullified the overall optical dispersion presented by the link.

In-line phase conjugation has also been applied for mitigation of intrachannel nonlinear effects [72]. Using a standard positive/negative dispersion map per span to ensure that the phase conjugation will primarily address intrachannel nonlinear effects, along with counterpropagating Raman amplification to balance the optical power on each side of the PPLN waveguide, significant reach extension was possible using the PPLN waveguide-based phase conjugator. In this demonstration, 100%, 33%, and 25% reach extension was realized for 40-Gb/s carrier-suppressed return-to-zero (CSRZ), NRZ, and RZ-DPSK signals, respectively, using the PPLN as a midspan nonlinearity compensator.

In one recent demonstration [73] of a phase-coded optical code-division multiple-access (OCDMA) system, the phase-preserving nature of SHG within a PPLN waveguide was used to determine the signal's correlation to the receiver's phase code. At the OCDMA transmitter, the "upper half" of the frequency spectrum of pulses from a femtosecond mode-locked laser was assigned phase codes using a pulse shaper and liquid crystal modulator. At the receiver, a user's OCDMA decoder applied a secondary set of phase codes to the "lower half" of the frequency spectrum of incoming pulses using similar hardware. The resulting pulse was sent through a PPLN waveguide to undergo SHG. In the case of complementary codes (the decoder is matched to the encoder), an SH output pulse is generated due to matching phase information across the pulse's frequency spectrum, and the transmitted data can be recovered. However, for an unmatched decoder, the pulse is not properly phasematched, and little-to-no SH output is recorded. Using this technique, $>$ 13-dB cross-correlation suppression was achieved. PPLN waveguides have also been used in other variations of nonlinear thresholding [74] applications.

### *C. Miscellaneous Applications*

The unique properties of the nonlinear processes that occur in a PPLN waveguide and the ability to control them at bit-time scales have led to their use in a diverse set of applications. This section touches on some of these applications that are difficult to classify under specific signal-processing domains.

*1) Two-dimensional (2-D) OCDMA Code Converter:* In a 2-D OCDMA architecture [75], [76], each bit is subdivided into a combination of chip times and a discrete set of wavelengths. Networks based on OCDMA may benefit greatly from an all-optical code converter that would enable resolution of code contention while data is being transferred between local area networks (LANs). Such a module would also enable code reuse allowing communication4 in large LANs with a smaller number of total codes. One of the proposed implementations of an OCDMA code converter involves code translation in the wavelength domain using a PPLN waveguide and in the time domain using FBGs [77]. The PPLN waveguide plays a

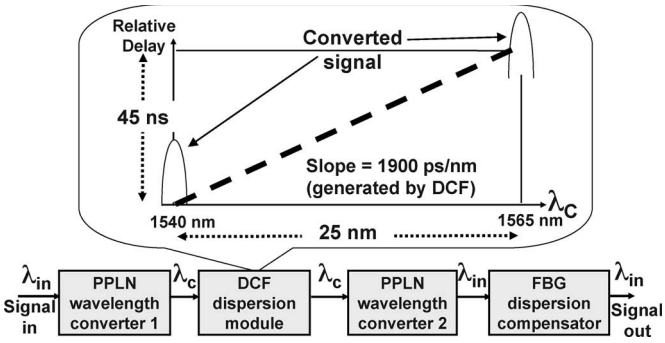


Fig. 20. Block diagram of tunable optical delay line based on PPLN waveguide wavelength converters and DCF. Using SFG/DFG, any input wavelength can be converted to the required new wavelength to experience a predetermined interchannel dispersion-induced time delay.

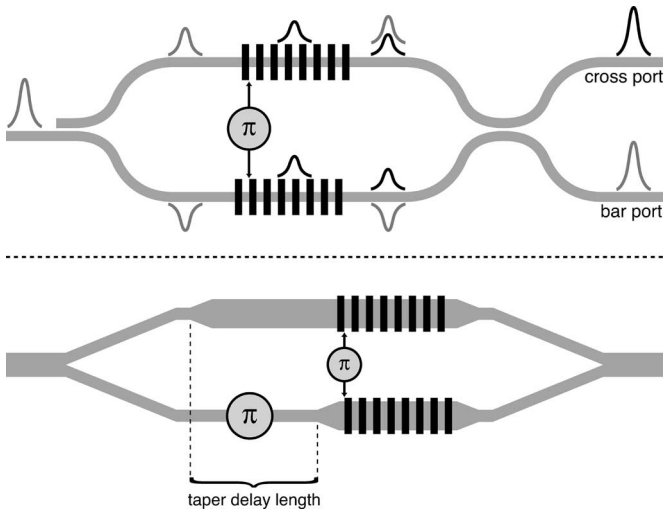


Fig. 21. OF balanced mixer implemented using symmetric Y-junctions.

critical role because it enables simultaneous conversion of all the wavelengths that form the chips of the coded OCDMA data.

*2) High-Speed TDM Multiplexing:* Single-channel data rates have been growing rapidly as techniques to mitigate fiber-based degradations are being successfully implemented. Generation of TDM channels at speeds in excess of 40 Gb/s requires optical multiplexing. A hybrid planar-lightwave-circuit (PLC)-based optical TDM multiplexer (OTDM-MUX) has been reported in [78]. The PLC-OTDM-MUX utilizes mixing in PPLN waveguides to modulate a pulse train all-optically, thereby imprinting the incoming data from multiple channels onto a single-output data stream. With this device, eight 20-Gb/s optical signals were multiplexed into a 160-Gb/s OTDM signal in a stable manner. This all-optical modulation scheme eliminates the microwave crosstalk between adjacent channels, which occurs in conventional electrooptic modulation schemes. There have also been other reports of PPLN devices being operated with single-channel speeds up to 160 Gb/s [50] and $4 \times 40$ Gb/s PLC-OTDM-MUX experiments [3].

*3) Tunable Optical Delay Line:* Tunable optical delays may see use in optical buffering [79], logic, synchronization, and equalization techniques. Conventional tunable optical delay lines consist of an optical switch and a loop of fiber. Optical data is switched into the loop and circulates through the loop until such time as the data need be released [80], when the switch can reroute data back into the network. However, due to the static nature of the loop, the resulting delay can only be an integer multiple of a single loop delay.

A recent demonstration [81] showed a continuously tunable (up to 44-ns maximum delay) optical delay line using a PPLN waveguide wavelength converter. A block diagram of this optical delay line is shown in Fig. 20. A PPLN waveguide wavelength converter is used to convert an input signal to a wavelength determined by the desired optical delay. (By using "dummy" pump wavelengths, the converted output wavelength can be chosen without changing the input wavelength.) After the converter, the signal is transmitted through a spool of dispersion-compensating fiber (DCF). Due to the high dispersion value ($-1900$ ps/nm) of the DCF spool, the signal experiences a relative time delay depending on the conversion wavelength, from 0 to $\sim$ 44 ns. A second PPLN waveguide wavelength converter then restores the signal to the original input wavelength, and an FBG is used to compensate for any intrachannel dispersion effects from the DCF spool. The result is an optical delay line for which the delay is continuously tunable without any significant signal distortion.

The unique properties of PPLN waveguides have led to their use in a wide variety of applications. As novel integrated structures based on PPLN waveguides emerge, new avenues will present themselves for the development of optical signal-processing technologies. Some of these key advances are discussed in the next section.

## IV. Advanced Device Concepts

Two problems that are common to simple parametric mixers described so far are 1) the inability to operate at degeneracy and 2) the speed limitations associated with the group-velocity mismatch (GVM). In this section, we discuss device architectures more complex than the implementations previously described, which address these issues.

The indistinguishability of input and output modes in conventional OF mixers requires separation via spectral filtering, precluding operation at degeneracy. Two device designs that address this issue have been demonstrated. One takes its inspiration from the balanced mixer techniques common in RF technology. A schematic of such an OF balanced mixer is shown in Fig. 21(a). The input is split into the two arms of a Mach–Zehnder interferometer and mixed with the pump to generate output signals nominally identical in magnitude. By fabricating the QPM gratings so that they are shifted by a half period in the two arms of the interferometer, the output signals in the two arms are $\pi$ out of phase with each other and, hence, exit from the cross rather than the bar port of the interferometer. A more convenient implementation with Y-junctions rather than 3-dB couplers [Fig. 21(b)] operates on the same principle but, as it has a single output, requires that a $\pi$ phase shift be introduced between the two arms by fabricating a portion of one of the arms with a slightly different waveguide. A proof of principle version of this device showed 13-dB rejection of pump and signal from the output port. Although more precisely controlled fabrication could yield devices with better contrast,

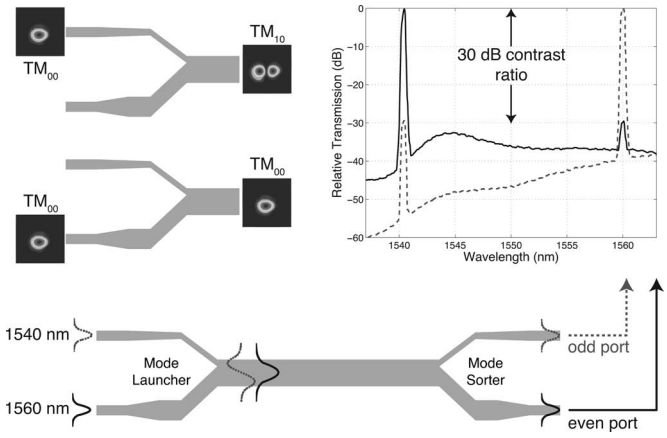


Fig. 22. Experimental data showing 3-dB contrast ratio between odd and even ports of asymmetric Y-junction device.

it will always be limited by the degree to which splitting ratios and mixing efficiency can be matched in the two arms.

An approach that avoids these problems is shown in Fig. 22, which relies only on adiabatic mode evolution to ensure high contrast between output and inputs. In this device, mixing takes place between inputs and outputs in different spatial modes of the two-mode waveguide. With the arms of an asymmetric Y-junction (termed the even and odd ports), it is possible to selectively excite the fundamental and first higher order mode of the waveguide and to similarly selectively separate modes at the output [82]. With the inputs launched into the even modes of the waveguide, and the output generated in the odd mode, they are separated at the output Y-junction with a contrast that depends only on the adiabatic evolution of the modes. We have observed 30-dB contrast in such asymmetric Y-junction mode filters [83]. This same approach can be used in high-contrast switches, background-free autocorrelators, spatial separation of degenerate photon pairs, etc.

Limits on the pulse durations that can be generated in a given length OF mixer (or equivalently upper limits on the useful length of an OF mixer designed to operate with a given length pulse) are imposed by GVM between the interacting wavelengths. This can be readily understood by looking at the case of pulsed SHG. Inasmuch as the group velocities of the fundamental and second harmonic fields differ by $\delta v = 1/v_{2\omega} - 1/v_{\omega}$, the GVM parameter, they will walk off of each other as they propagate down the waveguide. This walk-off will result in a distortion of the generated SH field, effectively stretching it in time. For the important 1550/775-nm first harmonic FH/SH pair, $\delta v \approx 0.35$ ps/mm in a standard RPE PPLN waveguide, limiting the usable effective conversion length to 3 cm in a system using 10-ps long pulses. Although we cannot change the group velocities in any significant way by modifying the dispersion in these weakly guiding waveguides, the use of directional couplers and delay lines allows us to retime the FH and SH fields on-chip as shown in Fig. 23. After delaying the faster pulse envelope, propagation through a second-conversion section allows continued additive SH generation without GVM-induced pulse distortion. The effectively doubled interaction length increases the SHG efficiency by a factor of 4, whereas

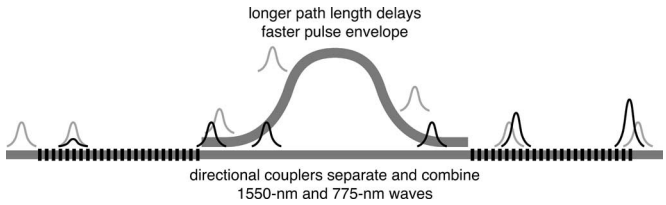


Fig. 23. GVM compensation scheme. The fundamental wave (gray) is delayed with respect to the second harmonic (black).

cascaded processes gain a factor of 16 in efficiency. Repeated application of this quasi-GVM (QGVM) structure allows for a significant increase in the converted energy and therefore the overall device performance [84].

## V. Conclusion

In this paper, we reviewed all-optical signal processing in $\chi^{(2)}$-based guided-wave devices, focusing on APE/RPE PPLN waveguides. Various applications in digital optical and phase-based signal processing were reviewed, as well as a number of applications in OCDMA and OTDM at speeds up to 160 Gb/s. The development of new integrated components such as two-mode mixers based on asymmetric Y-junctions and QGVM structures will allow the realization of previously inaccessible signal-processing functions. It has been shown that $\chi^{(2)}$-based devices can deliver strictly transparent signal processing at speeds beyond 1 Tb/s. With the advent of dense WDM (DWDM) networks operating beyond 160 Gb/s, all-optical signal processing can play a role in future network designs.

## References

[1] C. A. Brackett, "Dense wavelength division multiplexing networks: Principles and applications," *IEEE J. Sel. Areas Commun.*, vol. 8, no. 6, pp. 948–964, Aug. 1990.

[2] S. J. B. Yoo, "Wavelength conversion technologies for WDM network applications," *J. Lightw. Technol.*, vol. 14, no. 6, pp. 955–966, Jun. 1996.

[3] T. Ohara, H. Takara, I. Shake, K. Mori, K. Sato, S. Kawanishi, S. Mino, I. Yamada, A. Ishii, I. Ogawa, T. Kitoh, K. Magari, A. Okamoto, R. V. Roussev, J. R. Kurz, K. R. Parameswaran, and M. M. Fejer, "160-Gb/s OTDM transmission using integrated all-optical MUX/DEMUX with all-channel modulation and demultiplexing," *IEEE Photon. Technol. Lett.*, vol. 16, no. 2, pp. 650–652, Feb. 2004.

[4] B. Chen, C.-Q. Xu, B. Zhou, Y. Nihei, and A. Harada, "All-optical variable-in variable-out wavelength conversions by using MgO:$LiNbO_3$ quasiphase matched wavelength converter," *Jpn. J. Appl. Phys.*, vol. 40, no. 12B, pp. L1370–L1372, Dec. 2001.

[5] M. H. Chou, I. Brener, G. Lenz, R. Scotti, E. E. Chaban, J. Shmulovich, D. Philen, S. Kosinski, K. R. Parameswaran, and M. M. Fejer, "Efficient wide-band and tunable midspan spectral inverter using cascaded nonlinearities in $LiNbO_3$ waveguides," *IEEE Photon. Technol. Lett.*, vol. 12, no. 1, pp. 82–84, Jan. 2000.

[6] H. Tan, G. P. Banfi, and A. Tomaselli, "Optical frequency mixing through cascaded second-order processes in $\beta$-barium borate," *Appl. Phys. Lett.*, vol. 63, no. 18, pp. 2472–2474, Nov. 1993.

[7] G. I. Stegeman, M. Sheik-Bahae, E. V. Stryland, and G. Assanto, "Large nonlinear phase shifts in second-order nonlinear-optical processes," *Opt. Lett.*, vol. 18, no. 1, pp. 13–15, Jan. 1993.

[8] G. I. Stegeman, D. J. Hagan, and L. Torner, "$\chi^{(2)}$ cascading phenomena and their applications to all-optical signal processing, mode-locking, pulse compression and solitons," *Opt. Quantum Electron.*, vol. 28, no. 12, pp. 1691–1740, Dec. 1996.

[9] T. Suhara and M. Fujimura, *Waveguide Nonlinear-Optic Device,* ser. Springer Series in Photonics. Berlin, Germany: Springer-Verlag, 2003.

[10] M. L. Bortz, S. J. Field, M. M. Fejer, D. W. Nam, R. G. Waarts, and D. F. Welch, "Noncritical quasi-phase-matched second harmonic

generation in an annealed proton-exchanged $LiNbO_3$ waveguide," *IEEE J. Quantum Electron.*, vol. 30, no. 12, pp. 2953–2960, Dec. 1994.

[11] M. H. Chou, J. Hauden, M. A. Arbore, and M. M. Fejer, "1.5-$\mu$m-band wavelength conversion based on difference-frequency generation in $LiNbO_3$ waveguides with integrated coupling structures," *Opt. Lett.*, vol. 23, no. 13, pp. 1004–1006, Jul. 1998.

[12] K. Gallo, G. Assanto, and G. I. Stegeman, "Efficient wavelength shifting over the erbium amplifier bandwidth via cascaded second order processes in lithium niobate waveguides," *Appl. Phys. Lett.*, vol. 71, no. 8, pp. 1020–1022, Aug. 1997.

[13] K. Gallo and G. Assanto, "Analysis of lithium niobate all-optical wavelength shifters for the third spectral window," *J. Opt. Soc. Amer. B, Opt. Phys.*, vol. 16, no. 5, pp. 741–753, May 1999.

[14] P. K. Tien, R. Ulrich, and R. J. Martin, "Optical second harmonic generation in form of coherent Cerenkov radiation from a thin-film waveguide," *Appl. Phys. Lett.*, vol. 17, no. 6, pp. 447–449, Jun. 1970.

[15] E. J. Lim, M. M. Fejer, R. L. Byer, and W. J. Kozlovsky, "Blue light generation by frequency doubling in a periodically poled lithium niobate channel waveguide," *Electron. Lett.*, vol. 25, no. 11, pp. 731–732, May 1989.

[16] M. M. Fejer, *Nonlinear Frequency Conversion in Periodically-Poled Ferroelectric Waveguides*, D. B. Ostrowsky and R. Reinisch, Eds. Norwell, MA: Kluwer, 1992.

[17] C. Q. Xu, H. Okayama, and M. Kawahara, "1.5-$\mu$m band efficient broadband wavelength conversion by difference frequency generation in a periodically domain-inverted $LiNbO_3$ channel waveguide," *Appl. Phys. Lett.*, vol. 63, no. 26, pp. 3559–3561, Dec. 1993.

[18] C. Q. Xu, H. Okayama, K. Shinozaki, K. Watanabe, and M. Kawahara, "Wavelength conversions approximately 1.5-$\mu$m by difference frequency generation in periodically domain-inverted $LiNbO_3$ channel waveguides," *Appl. Phys. Lett.*, vol. 63, no. 9, pp. 1170–1172, Aug. 1993.

[19] C. Q. Xu, H. Okayama, and M. Kawahara, "Wavelength conversions between the two silica fibre loss windows at 1.31 and 1.55-$\mu$m using difference frequency generation," *Electron. Lett.*, vol. 30, no. 25, pp. 2168–2169, Dec. 1994.

[20] M. L. Bortz, D. Serkland, and M. M. Fejer, "Near degenerate difference frequency generation at 1.3-$\mu$m in $LiNbO_3$ waveguides for application as an all-optical channel shifter," in *Proc. CLEO/IQEC*, Anaheim, CA, May 8–13, 1994, pp. 288–289.

[21] S. J. B. Yoo, R. Bhat, C. Caneau, and M. A. Koza, "Quasi-phase-matched second-harmonic generation in AlGaAs waveguides with periodic domain inversion achieved by wafer-bonding," *Appl. Phys. Lett.*, vol. 66, no. 25, pp. 3410–3412, Jun. 1995.

[22] S. J. B. Yoo, C. Caneau, R. Bhat, M. A. Koza, A. Rajhel, and N. Antoniades, "Wavelength conversion by difference frequency generation in AlGaAs waveguides with periodic domain inversion achieved by wafer bonding," *Appl. Phys. Lett.*, vol. 68, no. 19, pp. 2609–2611, May 1996.

[23] K. R. Parameswaran, R. K. Route, J. R. Kurz, R. V. Roussev, M. M. Fejer, and M. Fujimura, "Highly efficient second-harmonic generation in buried waveguides formed by annealed and reverse proton exchange in periodically poled lithium niobate," *Opt. Lett.*, vol. 27, no. 3, pp. 179–181, Feb. 2002.

[24] G. D. Miller, R. G. Batchko, M. M. Fejer, and R. L. Byer, "Visible quasi-phase-matched harmonic generation by electric-field-poled lithium niobate," in *Proc. SPIE—Int. Society Optical Engineering*, 1996, vol. 2700, pp. 34–45.

[25] M. L. Bortz and M. M. Fejer, "Measurement of the second-order nonlinear susceptibility of proton-exchanged $LiNbO_3$," *Opt. Lett.*, vol. 17, no. 10, pp. 704–706, May 1992.

[26] Y. N. Korkishko, V. A. Fedorov, and F. Laurell, "The SHG-response of different phases in proton exchanged lithium niobate waveguides," *IEEE J. Sel. Topics Quantum Electron.*, vol. 6, no. 1, pp. 132–142, Jan. 2000.

[27] K. R. Parameswaran, M. Fujimura, M. H. Chou, and M. M. Fejer, "Low-power all-optical gate based on sum frequency mixing in APE waveguides in PPLN," *IEEE Photon. Technol. Lett.*, vol. 12, no. 6, pp. 654–656, Jun. 2000.

[28] J. L. Jackel and J. J. Johnson, "Reverse exchange method for burying proton exchanged waveguides," *Electron. Lett.*, vol. 27, no. 15, pp. 1360–1361, Jul. 1991.

[29] Y. Korkishko, V. A. Fedorov, T. M. Morozova, F. Caccavale, F. Gonella, and F. Segato, "Reverse proton exchange for buried waveguides in $LiNbO_3$," *J. Opt. Soc. Amer. B, Opt. Phys.*, vol. 15, no. 7, pp. 1838–1842, Jul. 1998.

[30] R. Roussev, A. Sridharan, K. Urbanek, R. Byer, and M. Fejer, "Parametric amplification of 1.6-$\mu$m signal in anneal- and reverse-proton exchanged waveguides," in *Proc. IEEE LEOS Annu. Meeting Conf.*, Oct. 2003, vol. 1, pp. 334–335.

[31] E. J. Lim, S. Matsumoto, and M. M. Fejer, "Noncritical phase matching for guided-wave frequency conversion," *Appl. Phys. Lett.*, vol. 57, no. 22, pp. 2294–2296, Nov. 1990.

[32] M. H. Chou, M. A. Arbore, and M. M. Fejer, "Adiabatically tapered periodic segmentation of channel waveguides for mode-size transformation and fundamental mode excitation," *Opt. Lett.*, vol. 21, no. 11, pp. 794–796, Jun. 1996.

[33] R. Roussev, X. Xie, K. Parameswaran, M. Fejer, and J. Tian, "Accurate semi-empirical model for annealed proton exchanged waveguides in $z$-cut lithium niobate," in *Proc. IEEE LEOS Annu. Meeting Conf.*, Oct. 2003, vol. 1, pp. 338–339.

[34] M. H. Chou, I. Brener, K. R. Parameswaran, and M. M. Fejer, "Stability and bandwidth enhancement of difference frequency generation DFG-based wavelength conversion by pump detuning," *Electron. Lett.*, vol. 35, no. 12, pp. 978–980, Jun. 1999.

[35] T. R. Volk, V. I. Pryalkin, and N. M. Rubinina, "Optical-damage-resistant $LiNbO_3$:Zn crystal," *Opt. Lett.*, vol. 15, no. 18, pp. 996–998, Sep. 1990.

[36] W. M. Young, R. S. Feigelson, M. M. Fejer, M. J. F. Digonnet, and H. J. Shaw, "Photorefractive-damage-resistant Zn-diffused waveguides in $MgO:LiNbO_3$," *Opt. Lett.*, vol. 16, no. 13, pp. 995–997, Jul. 1991.

[37] W. M. Young, M. M. Fejer, M. J. F. Digonnet, A. F. Marshall, and R. S. Feigelson, "Fabrication, characterization and index profile modeling of high-damage resistance Zn-diffused waveguides in congruent and MgO:lithium niobate," *J. Lightw. Technol.*, vol. 10, no. 9, pp. 1238–1246, Sep. 1992.

[38] K. Mizuuchi, K. Yamamoto, and M. Kato, "Harmonic blue light generation in $x$-cut $MgO:LiNbO_3$ waveguide," *Electron. Lett.*, vol. 33, no. 9, pp. 806–807, Apr. 1997.

[39] M. Asobe, H. Miyazawa, O. Tadanaga, Y. Nishida, and H. Suzuki, "A highly damage-resistant $Zn:LiNbO_3$ ridge waveguide and its application to a polarization-independent wavelength converter," *IEEE J. Quantum Electron.*, vol. 39, no. 10, pp. 1327–1333, Oct. 2003.

[40] Y. Nishida, H. Miyazawa, A. Asobe, O. Tadanaga, and H. Suzuki, "0-db wavelength conversion using direct-bonded QPM-$Zn:LiNbO_3$ ridge waveguide," *IEEE Photon. Technol. Lett.*, vol. 17, no. 5, pp. 1049–1051, May 2005.

[41] Y. L. Lee, H. Suche, Y. H. Min, J. H. Lee, W. Grundkotter, V. Quiring, and W. Sohler, "Wavelength- and time-selective all-optical channel dropping in periodically poled $Ti:LiNbO_3$ channel waveguides," *IEEE Photon. Technol. Lett.*, vol. 15, no. 7, pp. 978–980, Jul. 2003.

[42] W. Sohler, W. Grundkötter, D. Hofmann, I. Kostjucenko, S. Orlov, V. Quiring, R. Ricken, G. Schreiber, and H. Suche, "Integrated optical parametric oscillators with Ti:PPLN waveguides," in *Proc. CLEO Tech. Dig. Postconf. Edition*, Baltimore, MD, May 22–27, 2005, pp. 195–197.

[43] C. Q. Xu, H. Okyama, and T. Kamijoh, "Polarization insensitive wavelength conversions by a $LiNbO_3$ waveguide using a multi-ring configuration," *Opt. Rev.*, vol. 4, no. 5, pp. 546–549, Sep. 1997.

[44] I. Brener, M. H. Chou, E. Chaban, K. R. Parameswaran, M. M. Fejer, and S. Kosinski, "Polarization-insensitive parametric wavelength converter based on cascaded nonlinearities in $LiNbO_3$ waveguides," in *Proc. Opt. Fiber Commun. Conf. Tech. Dig. Postconf. Edition. Trends Opt. and Photon. Vol. 37,* Baltimore, MD, vol. 1, T. Li, Ed. Washington, DC: Opt. Soc. Amer., Mar. 7–10, 2000, pp. 66–68.

[45] M. H. Chou, K. R. Parameswaran, M. M. Fejer, and I. Brener, "Multiple-channel wavelength conversion by use of engineered quasi-phase-matching structures in $LiNbO_3$ waveguides," *Opt. Lett.*, vol. 24, no. 16, pp. 1157–1159, Aug. 1999.

[46] G. Imeshev, M. A. Arbore, M. M. Fejer, A. Galvanauskas, M. Fermann, and D. Harter, "Ultrashort-pulse second-harmonic generation with longitudinally nonuniform quasi-phase-matching gratings: Pulse compression and shaping," *J. Opt. Soc. Amer. B, Opt. Phys.*, vol. 17, no. 2, pp. 304–318, Feb. 2000.

[47] S. L. Jansen, D. van den Borne, B. Spinnler, S. Calabro, H. Suche, P. M. Krummrich, W. Sohler, G. D. Khoe, and H. de Waardt, "Optical phase conjugation for ultra long-haul phase-shift-keyed transmission," *J. Lightw. Technol.*, vol. 24, no. 1, pp. 54–64, Jan. 2006.

[48] S. L. Jansen, D. van den Borne, P. M. Krummrich, S. Spälter, H. Suche, W. Sohler, G. D. Khoe, and H. de Waardt, "Phase conjugation for increased system robustness," presented at the Proc. Conference Optical Fiber Communication, Anaheim, CA, Mar. 7–10, 2006, Paper OTuK3.

[49] I. Brener, B. Mikkelsen, G. Raybon, R. Harel, K. Parameswaran, J. Kurz, and M. M. Fejer, "Parametric wavelength conversion and phase conjugation in $LiNbO_3$ waveguides," in *Proc. IEEE Annu. Meeting Conf. LEOS*, Rio Grande, PR, vol. 2. Piscataway, NJ: IEEE, Nov. 13–16, 2000, pp. 766–767.

[50] I. Brener, B. Mikkelsen, G. Raybon, R. Harel, K. Parameswaran, J. R. Kurz, and M. M. Fejer, "160 Gb/s wavelength shifting and phase

conjugation using periodically poled $LiNbO_3$ waveguide parametric converter," *Electron. Lett.*, vol. 36, no. 21, pp. 1788–1790, Oct. 2000.

[51] S. L. Jansen, S. Spalter, G. D. Khoe, H. de Waardt, H. E. Escobar, L. Marshall, and M. Sher, "16 × 40 Gb/s over 800 km of SSMF using mid-link spectral inversion," *IEEE Photon. Technol. Lett.*, vol. 16, no. 7, pp. 1763–1765, Jul. 2004.

[52] J. E. McGeehan, M. Giltrelli, and A. E. Willner, "All-optical digital 3-input and gate using sum- and difference-frequency generation in a PPLN waveguide," in *Proc. Dig. LEOS Summer Top. Meetings*, Jul. 2005, pp. 179–180.

[53] S. Kumar, D. Gurkan, and A. E. Willner, "All-optical half adder using a PPLN waveguide and an SOA," presented at the Proc. Optical Fiber Communication Conference, vol. 1, Los Angeles, CA, Feb. 23–27, 2004, Paper WN2.

[54] D. J. Blumenthal, J. E. Bowers, L. Rau, H.-F. Chou, S. Rangarajan, W. Wang, and K. N. Poulsen, "Optical signal processing for optical packet switching networks," *IEEE Commun. Mag.*, vol. 41, no. 2, pp. S23–S29, Feb. 2003.

[55] T. Houbavlis, K. E. Zoiros, M. Kalyvas, G. Theophilopoulos, C. Bintjas, K. Yiannopoulos, N. Pleros, K. Vlachos, H. Avramopoulos, L. Schares, L. Occhi, G. Guekos, J. R. Taylor, S. Hansmann, and W. Miller, "All-optical signal processing and applications within the esprit project DO_ALL," *J. Lightw. Technol.*, vol. 23, no. 2, pp. 781–801, Feb. 2005.

[56] V. Paxson, "End-to-end routing behavior in the internet," *IEEE/ACM Trans. Netw.*, vol. 5, no. 5, pp. 601–615, Oct. 1997.

[57] J. E. McGeehan, S. Kumar, D. Gurkan, S. M. R. M. Nezam, A. E. Willner, K. R. Parameswaran, M. M. Fejer, J. Bannister, and J. D. Touch, "All-optical decrementing of a packet's time-to-live (TTL) field and subsequent dropping of a zero-TTL packet," *J. Lightw. Technol.*, vol. 21, no. 11, pp. 2746–2752, Nov. 2003.

[58] D. J. Blumenthal, B. E. Olsson, G. Rossi, T. E. Dimmick, L. Ran, M. Masanovi, O. Lavrova, R. Doshi, O. Jerphagnon, J. E. Bowers, V. Kaman, L. A. Coldren, and J. Barton, "All-optical label swapping networks and technologies," *J. Lightw. Technol.*, vol. 18, no. 12, pp. 2058–2075, Dec. 2000.

[59] B. Meagher, G. K. Chang, G. Ellinas, Y. M. Lin, W. Xin, T. F. Chen, X. Yang, A. Chowdhury, J. Young, S. J. Yoo, C. Lee, M. Z. Iqbal, T. Robe, H. Dai, Y. J. Chen, and W. I. Way, "Design and implementation of ultra-low latency optical label switching for packet-switched WDM networks," *J. Lightw. Technol.*, vol. 18, no. 12, pp. 1978–1987, Dec. 2000.

[60] F. Ramos, E. Kehayas, J. M. Martinez, R. Clavero, J. Marti, L. Stampoulidis, D. Tsiokos, H. Avramopoulos, J. Zhang, P. V. Holm-Nielsen, N. Chi, P. Jeppesen, N. Yan, I. T. Monroy, A. M. J. Koonen, M. T. Hill, Y. Liu, H. J. S. Dorren, R. V. Caenegem, D. Colle, M. Pickavet, and B. Riposati, "IST-LASAGNE: Towards all-optical label swapping employing optical logic gates and optical flip-flops," *J. Lightw. Technol.*, vol. 23, no. 10, pp. 2993–3011, Oct. 2005.

[61] A. Viswanathan, N. Feldman, Z. Wang, and R. Callon, "Evolution of multiprotocol label switching," *IEEE Commun. Mag.*, vol. 36, no. 5, pp. 165–173, May 1998.

[62] E. Rosen, A. Viswanathan, and R. Callon (2001). Multiprotocol label switching architecture. *Internet Engineering Task Force, Request for Comments (RFC) 3031*. [Online]. Available: http://www.ietf.org/rfc/rfc3031.txt?number=3031

[63] T. Fjelde, A. Kloch, D. Wolfson, B. Dagens, A. Coquelin, I. Guillemot, F. Gaborit, F. Poingt, and M. Renaud, "Novel scheme for simple label-swapping employing XOR logic in an integrated interferometric wavelength converter," *IEEE Photon. Technol. Lett.*, vol. 13, no. 7, pp. 750–752, Jul. 2001.

[64] S. J. B. Yoo, H. J. Lee, Z. Pan, J. Cao, Y. Zhang, K. Okamoto, and S. Kamei, "Rapidly switching all-optical packet routing system with optical-label swapping incorporating tunable wavelength conversion and a uniform-loss cyclic frequency AWGR," *IEEE Photon. Technol. Lett.*, vol. 14, no. 8, pp. 1211–1213, Aug. 2002.

[65] W. Hung, C.-K. Chan, L.-K. Chen, and F. Long, "Demonstration of an optical packet label swapping scheme using DPSK encoded bit-serial labels," in *Proc. 5th Pacific Rim Conference on Lasers and Electro-Optics (CLEO)*, Taipei, Taiwan, R.O.C., Dec. 15–19, 2003, vol. 1, p. 154.

[66] E. N. Lallas, N. Skarmoutsos, and D. Syvridis, "Coherent encoding of optical FSK header for all optical label swapping systems," *J. Lightw. Technol.*, vol. 23, no. 3, pp. 1199–1209, Mar. 2005.

[67] D. Gurkan, S. Kumar, A. E. Willner, K. R. Parameswaran, and M. M. Fejer, "Simultaneous label swapping and wavelength conversion of multiple independent WDM channels in an all-optical MPLS network using PPLN waveguides as wavelength converters," *J. Lightw. Technol.*, vol. 21, no. 11, pp. 2739–2745, Nov. 2003.

[68] D. Gurkan, M. C. Hauer, A. B. Sahin, Z. Pan, S. Lee, A. E. Willner, K. R. Parameswaran, and M. M. Fejer, "Demonstration of multi-wavelength all-optical header recognition using a PPLN and optical correlators," in *Proc. 27th Eur. Conf. Opt. Commun.*, vol. 3. Amsterdam, The Netherlands, Sep. 30–Oct. 4, 2001, pp. 312–313.

[69] H. S. Hinton, "Photonic switching fabrics," *IEEE Commun. Mag.*, vol. 28, no. 4, pp. 71–89, Apr. 1990.

[70] M. C. Cardakli, D. Gurkan, S. A. Havstad, A. E. Willner, K. R. Parameswaran, M. M. Fejer, and I. Brener, "Tunable all-optical time-slot-interchange and wavelength conversion using difference-frequency-generation and optical buffers," *IEEE Photon. Technol. Lett.*, vol. 14, no. 2, pp. 200–202, Feb. 2002.

[71] S. L. Jansen, D. van den Borne, C. Climent, M. Serbay, C. J. Weiske, H. Suche, P. M. Krummrich, S. Spalter, S. Calabro, N. Hecker-Denschlag, P. Leisching, W. Rosenkranz, W. Sohler, G. D. Khoe, T. Koonen, and H. de Waardt, "10,200 km 22 × 2 × 10 Gb/s RZ-DQPSK dense WDM transmission without inline dispersion compensation through optical phase conjugation," presented at the Proc. Optical Fiber Communication Conference Post Deadline Papers, vol. 5, Anaheim, CA, Mar. 6–11, 2005, Paper PDP28.

[72] A. Chowdhury, G. Raybon, R. J. Essiambre, J. H. Sinsky, A. Adamiecki, J. Leuthold, C. R. Doerr, and S. Chandrasekhar, "Compensation of intrachannel nonlinearities in 40-Gb/s pseudolinear systems using optical-phase conjugation," *J. Lightw. Technol.*, vol. 23, no. 1, pp. 1172–1177, Jan. 2005.

[73] Z. Zheng, A. M. Weiner, K. R. Parameswaran, M. N. Chou, and M. M. Fejer, "All-optical recognition of spectrally coded optical pulses using periodically poled lithium niobate second-harmonic waveguides for ultrashort pulse optical code division multiple-access," in *Proc. CLEO Tech. Dig. Postconf. Edition TOPS*, San Francisco, CA, vol. 39. Salem, MA: Opt. Soc. Amer., May 7–12, 2000, pp. 194–195.

[74] Z. Jiang, D. S. Seo, S. D. Yang, D. E. Leaird, R. V. Roussev, C. Langrock, M. M. Fejer, and A. M. Weiner, "Four-user, 2.5-Gb/s, spectrally coded OCDMA system demonstration using low-power nonlinear processing," *J. Lightw. Technol.*, vol. 23, no. 1, pp. 143–158, Jan. 2005.

[75] L. Tancevski, I. Andonovic, M. Tur, and J. Budin, "Massive optical LANs using wavelength hopping/time spreading with increased security," *IEEE Photon. Technol. Lett.*, vol. 8, no. 7, pp. 935–937, Jul. 1996.

[76] H. Fathallah, L. A. Rusch, and S. LaRochelle, "Passive optical fast frequency-hop CDMA communications system," *J. Lightw. Technol.*, vol. 17, no. 3, pp. 397–405, Mar. 1999.

[77] D. Gurkan, S. Kumar, A. Sahin, A. Willner, K. Parameswaran, M. Fejer, D. Starodubov, J. Bannister, P. Kamath, and J. Touch, "All-optical wavelength and time 2-D code converter for dynamically-reconfigurable O-CDMA networks using a PPLN waveguide," in *Proc. OFC Tech. Dig.*, Atlanta, GA, vol. 32. Washington, DC: Opt. Soc. Amer., Mar. 23–28, 2003, pp. 654–656.

[78] T. Ohara, H. Takara, I. Shake, K. Mori, S. Kawanishi, S. Mino, T. Yamada, M. Ishii, T. Kitoh, T. Kitagawa, K. R. Parameswaran, and M. M. Fejer, "160-Gb/s optical-time-division multiplexing with PPLN hybrid integrated planar lightwave circuit," *IEEE Photon. Technol. Lett.*, vol. 15, no. 2, pp. 302–304, Feb. 2003.

[79] C. Guillemot, M. Renaud, P. Gambini, C. Janz, I. Andonovic, R. Bauknecht, B. Bostica, M. Burzio, F. Callegati, M. Casoni, D. Chiaroni, F. Clerot, S. L. Danielsen, F. Dorgeuille, A. Dupas, A. Franzen, P. B. Hansen, D. K. Hunter, A. Kloch, R. Krahenbuhl, B. Lavigne, A. L. Corre, C. Raffaelli, M. Schilling, J. C. Simon, and L. Zucchelli, "Transparent optical packet switching: The European ACTS KEOPS project approach," *J. Lightw. Technol.*, vol. 16, no. 12, pp. 2117–2134, Dec. 1998.

[80] T. Sakamoto, K. Noguchi, R. Sato, A. Okada, Y. Sakai, and M. Matsuoka, "Variable optical delay circuit using wavelength converters," *Electron. Lett.*, vol. 37, no. 7, pp. 454–455, Mar. 2001.

[81] Y. Wang, C. Yu, L. Yan, A. E. Willner, R. Roussev, C. Langrock, and M. M. Fejer, "Continuously-tunable dispersionless 44-ns all optical delay element using a two-pump PPLN, DCF, and a dispersion compensator," in *Proc. 31st Eur. Conf. Opt. Commun.*, Glasgow, U.K., vol. 4. Stevenage, U.K.: IEE, Sep. 25–29, 2005, pp. 793–794.

[82] H. Yajima, "Dielectric thin-film optical branching waveguide," *Appl. Phys. Lett.*, vol. 22, no. 12, pp. 647–649, Jun. 1973.

[83] J. R. Kurz, J. Huang, X. Xie, T. Saida, and M. M. Fejer, "Mode multiplexing in optical frequency mixers," *Opt. Lett.*, vol. 29, no. 6, pp. 551–553, Mar. 2004.

[84] J. Huang, J. R. Kurz, C. Langrock, and A. M. Schober, "Quasi-group-velocity matching using integrated-optic structures," *Opt. Lett.*, vol. 29, no. 21, pp. 2482–2484, Nov. 2004.

**Carsten Langrock** (S'01) received the diploma in physics from the Heinrich-Heine-Universitaet Duesseldorf, Duesseldorf, Germany, in 2001. He is currently working toward the Ph.D. degree in electrical engineering at Stanford University, Stanford, CA.

Currently, he is a Research Assistant in Prof. Martin M. Fejer's group in the Edward L. Ginzton Laboratory at Stanford University. His research interests include single-photon generation and detection, characterization of weak ultrashort optical pulses, and waveguide nonlinear optics.

Mr. Langrock is a Student Member of the IEEE Lasers and Electro-Optics Society and the Optical Society of America.

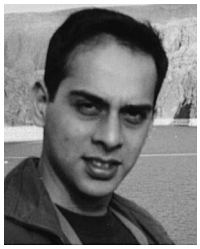

**Saurabh Kumar** (S'02) received the B.E. (Hons.) degree in electrical and electronics engineering from Birla Institute of Technology and Science, Pilani, India, in 2001 and the M.S. degree in electrical engineering from the University of Southern California (USC), Los Angeles, in 2003. He is currently working toward the Ph.D. degree in electrical engineering at the Optical Communications Laboratory, USC.

His research interests include all-optical signal processing, wavelength conversion, and optical routing functions for high-speed reconfigurable fiber-optic networks.

Mr. Kumar is a Student Member of the IEEE Lasers and Electro-Optics Society and the Optical Society of America. He is also a member of Eta Kappa Nu.

**John E. McGeehan** (S'96–M'04) received the B.S., M.S., and Ph.D. degrees from the University of Southern California, Los Angeles, in 1998, 2001, and 2005, respectively, all in electrical engineering. His doctoral research focused on routing and processing signals in wavelength-division-multiplexed optical communication networks.

He is currently a Senior Physicist at BAE Systems Advanced Technologies, Inc., Washington, DC. He has published more than 30 papers on the subjects of optically routed networks and polarization management. His current research areas include high-power optical systems without amplification and design of optically controlled high-power electrical semiconductor switches, as well as optical motor control, networks, and power management.

Dr. McGeehan is a member of the Optical Society of America.

**A. E. Willner** (S'87–M'88–SM'93–F'04) received the Ph.D. degree in electrical engineering from Columbia University, New York, NY, in 1988.

He has worked at AT&T Bell Laboratories and Bellcore. He is currently a Professor of electrical engineering at the University of Southern California (USC), Los Angeles. He has 525 publications, including one book.

Prof. Willner is a Fellow of the Optical Society of America and was a Fellow of the Semiconductor Research Corporation. His professional activities have included the following: President of the IEEE Lasers and Electro-Optics Society (LEOS), Editor-in-Chief of the IEEE/Optical Society of America (OSA) JOURNAL OF LIGHTWAVE TECHNOLOGY, Editor-in-Chief of the IEEE JOURNAL OF SELECTED TOPICS IN QUANTUM ELECTRONICS, Co-Chair of the OSA Science and Engineering Council, General Co-Chair of the Conference on Lasers and Electro-Optics (CLEO), General Chair of the LEOS Annual Meeting Program, Program Co-Chair of the OSA Annual Meeting, and Steering and Program Committee Member of the Conference on Optical Fiber Communications (OFC). He has received the National Science Foundation (NSF) Presidential Faculty Fellows Award from the White House, the Packard Foundation Fellowship, the NSF National Young Investigator Award, the Fulbright Foundation Senior Scholars Award, the IEEE LEOS Distinguished Traveling Lecturer Award, the USC University-Wide Award for Excellence in Teaching, the Eddy Award from Pennwell for the Best Contributed Technical Article, and the Armstrong Foundation Memorial Prize.

**M. M. Fejer** received the B.A. degree in physics from Cornell University, Ithaca, NY, in 1977 and the Ph.D. degree in applied physics from Stanford University, Stanford, CA, in 1986.

He is currently a Professor of applied physics and the Senior Asociate Dean for Natural Sciences at Stanford University. He has over 275 publications and 25 patents. His research interests include micro- and nanostructured materials, nonlinear and guided-wave optics, and optical signal-processing devices.

Prof. Fejer is a Fellow of the Optical Society of America. His professional activities have included the following: Membership on the Lasers and Electro-Optics Society (LEOS) and Optical Society of America (OSA) Boards of Directors, Chair of the OSA Quantum Electronics Division, and General Co-Chair of the Conference on Lasers and Electro-Optics (CLEO). He was the recipient of R. W. Wood Prize in 1998.